Scientific Papers. Series E. Land Reclamation, Earth Observation & Surveying, Environmental Engineering. Vol. XIII, 2024
Print ISSN 2285-6064, CD-ROM ISSN 2285-6072, Online ISSN 2393-5138, ISSN-L 2285-6064

APPLICATION OF MACHINE LEARNING APPROACHES FOR LAND USE CHANGE MODELLING IN SURINAME

Tamara MYSLYVA[1], Marciano DASAI[1], Christiaan Max HUISDEN[2], Petro NADTOCHIY[3], Yurii BILYAVSKYI[4]

[1]Ministry of Spatial Planning and Environment of Suriname,
22 Prins Hendrikstraat, Paramaribo, Republic of Suriname
[2]Anton de Kom University of Suriname, Leysweg, 86 Paramaribo, Republic of Suriname
[3]Institute of Agriculture of Polissia NAAS of Ukraine,
132 Kyiv highway, Zhytomyr, Ukraine
[4]Zhytomyr Agricultural Technical Professional College,
96 Pokrovska Street, Zhytomyr, Ukraine

Corresponding author email: byrty41@yahoo.com

Abstract

Machine learning (ML) algorithm-based models represent cutting-edge techniques used for mapping, quantifying, and modelling changes in land use and land cover (LULC) over time. In this study, a comparative analysis was conducted on the multilayer perceptron neural network (MLP) and support vector machine classification (SVM) applied to LULC change detection and forecasting within the coastal plain territory of Suriname. Sentinel-2A satellite data covering the period from 2017 to 2022 was utilised, along with additional variables such as the distance from rivers, roads, and administrative cities in each district and slope and digital elevation models in the prediction models. The SVM algorithm based predictive model, incorporating an urbanization transition sub-model, exhibited an impressive accuracy of 83.85%, surpassing the MLP algorithm-based model, which did not exceed 64.63%. Consequently, this model is recommended for generating LULC change prediction maps. These maps can serve as a crucial baseline for the Surinamese government, providing valuable insights for policy development and sustainable land use management.

Key words*: detection, machine learning, modelling, remote sensing, Suriname.*

INTRODUCTION

Analysing spatiotemporal trends in land use and land cover (LULC) change is crucial for gaining insights into effective and sustainable land management (Girma et al., 2022; Devi & Shimrah, 2023). This is particularly pertinent given the widespread prevalence of extensive LULC changes globally, especially in developing countries, where such transformations have become notably common in recent decades (Kafy et al., 2021). Similarly, Suriname has experienced pronounced LULC changes in the last decades, marked by a significant expansion of built-up areas at the expense of other LULC types, predominantly forest-covered and agricultural lands. Specifically, Suriname is struggling with illegal artisanal gold mining, causing large-scale contamination in the environment (Huisden et al., 2020a), as well as illegal deforestation that endangers biodiversity, degrades air and water quality, and leads to undesirable land use changes (Huisden et al., 2020b). LULC change modelling is an innovative technique for monitoring and managing land resources (Anurag & Pradhan, 2018) and has proven to be an essential tool for land use forecasting (Rozario et al., 2017). Modelling demonstrates the capability to efficiently represent and forecast complex LULC systems by incorporating multiple variables (Wang et al., 2021). These driving variables are represented by various geospatial data, which can be acquired through the use of satellite remote sensing data and geographical information system techniques (Kafy et al., 2021). Frequently employed models for predicting changes in land use encompass statistical models (Hyandye 2015; Yeh & Liaw, 2021), evolutionary models (Aitkenhead & Alders, 2009), cellular models (Muhammad et al., 2021), Markov models (Mohamed & Worku, 2020), hybrid models (Marquez et al., 2019), and multi-agent-based models (Ralha et al., 2013). Among these, the most widely utilised

are cellular and Markov chain analyses, along with their amalgamated form known as the CA-Markov model (Dey et al., 2021). Markov chain analysis, a random stochastic modelling method discrete in both time and state (Myslyva et al., 2021), outlines LULC transitions from one time period (t_1) to the next (t_2), enabling the projection of future changes (Rongqun et al., 2011). While Markov analysis is widely employed for simulating and predicting land use changes, it does have some drawbacks, making it more suitable for short-term projections (Sinha & Kumar, 2013). Notably, it lacks consideration for the spatial allocation of information within each class, and the probabilities of change between landscape states are not constant. As a result, while it can provide accurate magnitudes of change, it may not accurately indicate the direction of land use and land cover (LULC) changes (Wang et al., 2021). To augment the predictive capabilities of the Markov chain model, various techniques are implemented. Among these, a promising approach involves incorporating machine learning techniques, such as artificial neural networks or support vector machines, to complement the Markov model (Gharaibeh et al., 2020; Girma et al., 2022). This integration aims to enhance the model's capacity to capture intricate relationships and non-linear patterns in land-use change dynamics, thereby facilitating more accurate predictions of future land-use scenarios (Wang et al., 2021).

Despite the apparent occurrence of land use changes in the Suriname context, a notable gap exists in studies specifically addressing the detection of current trends and the prediction of future dynamics in the country's land use and land cover. This research void impedes a comprehensive understanding of the dynamic land use patterns in Suriname, limiting the ability to make informed decisions for sustainable development. Taking into account the aforementioned challenges, this study pursues a threefold objective: (1) to collect and process initial geospatial data on land use and land cover; (2) to evaluate the accuracy and reliability of two machine learning algorithms (MLP - multilayer perceptron neural network; SVM - support vector machine classification) in predicting future land use changes within Suriname; and (3) to develop a robust simulation model using the most effective machine learning algorithm identified from the comparative analysis. The simulation model is specifically designed to predict LULC changes over the upcoming 10-year period, aiming to provide valuable insights for strategic planning and decision-making in the context of Suriname's sustainable development.

MATERIALS AND METHODS

Study area. The studies were conducted in Suriname, a country situated north of the equator on the north-eastern coast of South America. Suriname's geographical coordinates extend from 1°50.45' N to 6°0.35' N and 53°59.08' W to 54°33.49' W. Geologically, over 80% of Suriname comprises the deeply weathered, rainforest-covered Precambrian Guiana Shield, extending east and south to the Amazon River in Brazil and west to the Orinoco River in Venezuela. Major rivers in the country include the Marowijne River, Commewijne River, Suriname River, Saramacca River, Coppename River, Nickerie River, and Corantijn River.

Suriname covers an area of approximately 16.4 million hectares and is divided into ten administrative districts, eight of which fall within the study area: Marowijne, Commewijne, Wanica, Paramaribo, Para, Saramacca, Coronie, and Nickerie (Figure 1). The study area, covering 25,755 km², is located in the northern part of Suriname within the Young Coastal Plain. This area ranges in width from about 20 km in the east to about 100 km in the west, with elevation variations of 0–4 m above mean sea level (MSL). Additionally, the study area includes the Old Coastal Plain, formed on remnants of ridges, gullies, and mud flats, with elevation variations of 4–10 m above MSL, and the Cover Landscape (also known as the Savannah Belt), ranging from 10 to 100 m above MSL (Ouboter & Jairam, 2012).

The climate of the study area is tropical-equatorial (Af), tropical monsoon (Am) and tropical savanna climate (Aw/As) (due to Köppen-Geiger climate classification). The average daily temperature varies from 26°C in January to 31°C in October. Average annual rainfall within the coastal plains ranges from 1500 to 1700 mm. The soil cover of the study area is represented by Umbric Glaysols, Albic

Arenosols, Albic Plintosols and Fibric Histosols according to the international soil classification system (WRB, 2014) (Gardi et al., 2015).

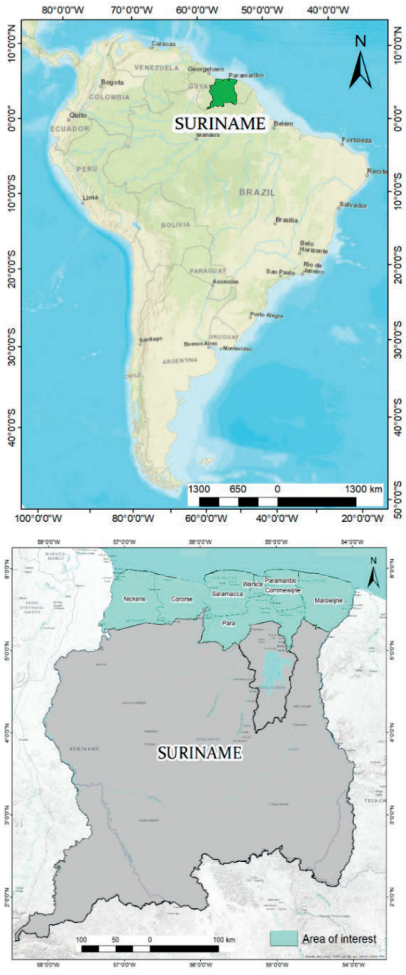

Figure 1. Location of the study area

Datasets used. In this study, three remotely sensed satellite images were employed to analyze LULC change dynamics. The Sentinel-2 L2A image scenes, which were classified and converted into LULC maps, were obtained from the freely accessible Esri land cover data portal. The downloaded raster images were pre-georeferenced in a latitude/longitude projection (EPSG:4326) with a datum and ellipsoid of WGS84. Additionally, the road-river network map and administrative cities of the district locations within the study area were acquired from OpenStreetMap (www.openstreetmap.org). The digital elevation model (DEM) was downloaded from the freely accessible 30-meter SRTM Tile Downloader (Table 1).

Table 1. Characteristics of data collected

Data	Source	Acquisition year	Scale/ Resolution
Multispectral satellite imagery	Esri Land Cover: https://livingatlas.arcgis.com/landcover/	2017 2021 2022	10 m
Digital Elevation Model	30-Meter SRTM Tile Downloader: https://dwtkns.com/srtm30m/	2018	1-arcsecond (3601x3601 pixels)

Slope, distance from rivers, distance from roads, and distance from urban datasets were developed through individual elaboration in 2023 with a resolution of 10 m.

These datasets underwent processing in QGIS 3.34 and ArcGIS 10.8 packages, involving operations such as projection to WGS 84 UTM Zone 21N, data conversion, DEM masking, and separation of road networks from other features (rivers) using the Query tool. The Euclidean distance function was employed to generate distance maps from roads, rivers/creeks, and urban areas using vector data of the features (Gharaibeh et al., 2020; Kafy et al., 2021). The DEM was manipulated in ArcGIS spatial analyst tools to create elevation and slope maps.

LULC change detection and simulation. Land Change Modeler (LCM) built in TerrSet software version 18.31 was utilized to detect and simulate future LULC changes. This empirically driven, stepwise process involves change analysis, transition potential modelling, and change prediction (Eastman, 2016), based on historical changes from time 1 (t_1 = 2017) to time 2 (t_2 = 2021). The Markov probability matrix was employed to determine the probability of converting from the current state (LULC class) to another state in the next period. Low and high transitions were assigned probabilities near 0 and 1, respectively (Sinha & Kumar, 2013; Wang et al., 2021). Gains and losses to each LULC category were identified, and transitions from one land cover state to another were used to generalize the spatial changing pattern (Dey et al., 2021; Leta et al.,

2021). Recognizing the need to incorporate the potential influence of independent variables in simulating LULC changes (Gharaibeh et al., 2020), this study considered six key driver variables. These variables include distances from rivers/creeks, roads, and administrative centres within the district, as well as terrain relief and slope represented by the DEM. Land cover transition potentials, indicating the likelihood of land transitioning from one class to another in the future, were determined using various methodologies, including a multi-layer perceptron neural network and support vector machine learning algorithms. Driver variables were inputted into the LCM transition sub-model, and machine learning algorithms were employed to generate potential transition maps using the dependent variables (2017 and 2021 imagery). Subsequently, hard predictions for the LULC changes in the year 2022 were generated. For every modelling approach, four transition sub-models were tested.

Validation of model outputs. The validation process was conducted to assess the agreement and disagreement between the actual and simulated LULC maps of 2022, ensuring the reliability and acceptance of different model approaches in predicting the future scenario in 2026 and 2031 (Dey et al., 2021; Kafy et al., 2021). Two distinct validations were carried out using the VALIDATE module in TerrSet and the ROC Tool of ArcSDM. The VALIDATE module computed kappa index statistics using the hard prediction as a comparison map, including kappa for no information (K_{no}), kappa for grid cell level location ($K_{location}$), kappa for stratum-level location ($K_{locationStrata}$), and kappa standard ($K_{standard}$) (Mishra et al., 2018; Girma et al., 2022). A strong and acceptable Kappa value is typically associated with values around 80% and above (Gharaibeh et al., 2020; Girma et al., 2022). The second method employed for estimating LULC change model performance was the Receiver Operating Characteristic (ROC). The area under the ROC curve (AUC) was calculated, representing the discriminatory power of the model in accurately predicting the occurrence or non-occurrence of land use change (Arabameri et al., 2019; Arora et al., 2021). AUC values were interpreted as follows: <0.6 (poor), 0.6-0.7 (moderate), 0.7-0.8 (good), 0.8-0.9 (very good), and >0.9 (excellent) model performance (Nhu et al., 2020). For future predictions, the images of 2017 and 2021 were considered as the dependent variables to simulate the LULC maps of 2026 and 2031. Figure 2 illustrates the modelling and validation processes employed in this study.

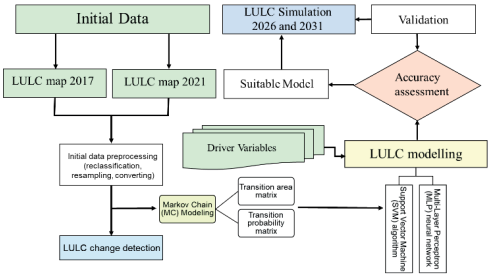

Figure 2. Research design flowchart

RESULTS AND DISCUSSIONS

Analyzing and comprehending the historical alterations in LULC dynamics is essential for predicting forthcoming trends in the coming decades (Regasa et al., 2021; Girma et al., 2022). The study area underwent landscape modifications, and diverse land use changes were observed during the period spanning from 2017 to 2021, as illustrated in Table 2 and Figure 3. Despite the overall stability in the structure of land cover, with over 80% of the territory remaining forested, a discernible trend was noted in the increase of flooded areas, constituting a net change of 25.7% of the total area.

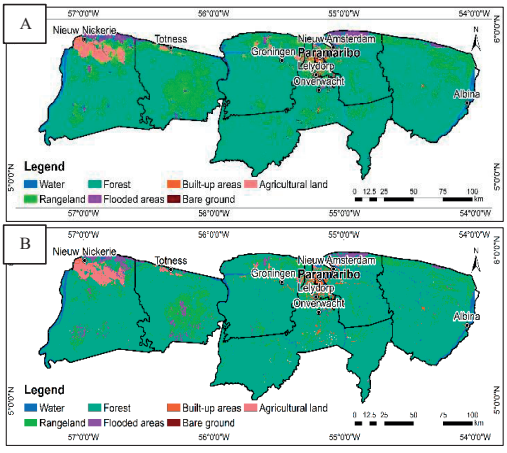

Figure 3. LULC maps for 2017 (A) and 2021 (B)

Several factors may contribute to the increase in flooded areas in Suriname: (a) changes in precipitation patterns and increased rainfall intensity due to global climate change; (b) human activities, such as deforestation, urbanization, or changes in agricultural practices, can alter or block natural waterways; (c) poorly designed or maintained drainage and flood control infrastructure.

Table 2. Area and net change of LULC classes

LULC class	Area, ha		Annual change, ha/year	Net change, % of area
	2017	2021		
Water	63755.9	66927.6	792.9	5.0
Forest	2112756.7	2146469.8	8428.3	1.6
Flooded areas	42030.8	52824.5	2698.4	25.7
Agricultural land	64147.9	59966.0	-1045.5	-6.5
Built-up areas	33765.8	37060.2	823.6	9.8
Bare ground	7370.4	266.9	-1775.9	-96.4
Rangeland	251705.8	212018.2	-9921.9	-15.8

Anthropogenic activities related to the development of buildings and constructions, especially intensive in coastal regions, coupled with uncontrolled and unjustified impacts on the hydrological regime, have played a crucial role in the rise of flooded areas. This is evidenced by a rapid annual increase in built-up areas, exceeding 820 hectares during the observation period. Gains and losses for the respective study period were acquired from the TerrSet LCM change analysis module and represented by a graph in Figures 4 and 5. The most significant increase occurred in forest-covered areas, while rangeland experienced a notable decrease throughout the entire period. The transitional area matrix contains the pixel number that is expected to change from each LULC class over the specified time frame (Eastman, 2016). Table 3 represents the detailed transition area matrix of each LULC class between 2017 and 2021.

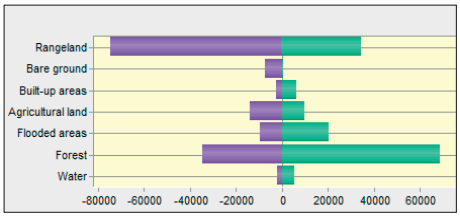

Figure 4. Gains and losses graph between 2017 and 2021 (ha)

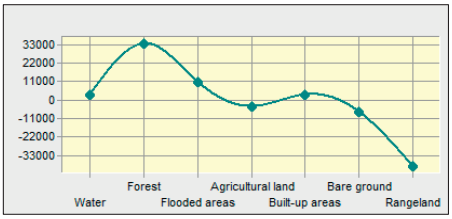

Figure 5. Net change graph between 2017 and 2021 (ha)

Table 3. Transition area matrix (thousand ha) of LULC between 2017 and 2021

2017	2021							Total
	Water	Forest	Flooded areas	Agricultural land	Built-up areas	Bare ground	Rangeland	
Water	61.5	1.2	0.6	0.1	0.0	0.0	0.3	63.8
Forest	2.2	2078.0	5.4	2.3	1.8	0.0	23.1	2112.8
Flooded areas	0.9	5.7	32.4	0.3	0.0	0.0	2.7	42.0
Agricultural land	0.7	3.7	2.5	50.1	0.5	0.0	6.7	64.1
Built-up areas	0.0	1.7	0.0	0.3	31.1	0.0	0.6	33.8
Bare ground	1.2	2.0	0.1	0.2	2.4	0.2	1.4	7.4
Rangeland	0.4	54.3	12.0	6.6	1.3	0.0	177.2	251.7
Total	66.9	2146.5	52.8	60.0	37.1	0.3	212.0	2575.5

In summary, there are notable changes in forest-covered and flooded areas, agricultural land, built-up areas, bare ground, and rangeland over the specified period. Rangeland, in particular, stands out with a considerable reduction, while forest and agricultural land show substantial increases. The outcomes of the LULC change analysis serve as the foundation for constructing transition sub-models. Based on these results, considering the most significant gains and losses for each land use class, four sub-transition models are identified (Table 4).

The factors influencing changes in land use are identified through spatial analysis and incorporated into the model as either static or dynamic components to enhance its accuracy (Leta et al., 2021). This study utilized topography and proximity factors for predicting LULC changes. Before integrating these drivers into the predictive model, selected driver variables underwent testing to assess their explanatory power, with Cramer's V used to

measure the strength of association and P values used for statistical significance evaluation (Table 5).

Table 4. Transition sub-models and their descriptors

Transition sub-model	Description	Land cover transition
Afforestation	Other land classes are converted to forest	Rangeland to forest Agricultural land to forest Bare ground to forest
Urbanization	Other land classes are converted to built-up areas	Bare ground to built-up areas Rangeland to built-up areas Agricultural land to built-up areas Forest to built-up areas
Flood intensification	Other land classes are converted to flooded areas or flooded areas are converted to water	Rangeland to flooded areas Agricultural land to flooded areas Flooded areas to water
Desolation	Agricultural land converted into other land classes	Agricultural land to flooded areas Agricultural land to built-up areas Agricultural land to forest Agricultural land to water

Table 5. Cramer's V and p-value for each of the explanatory variables

Driver variables	Cramer's V	p-value
Elevation	0.388	0.0000
Slope	0.379	0.0000
Distance from rivers	0.149	0.0000
Distance from roads	0.140	0.0000
Distance from urban	0.214	0.0000
Evidence Likelihood	0.763	0.0000

According to Eastman (2016), Cramer's V values of 0.15 or higher are considered 'useful,' while values of 0.4 or higher are deemed 'good.' Variables such as elevation, slope, and distance from rivers and urban areas are considered useful for predicting transitions. On the other hand, variables like distance from roads have low Cramer's V values, indicating that their effect on LULC change in the study area is not critical. The assessment of evidence likelihood serves as a means to determine the relative frequency of pixels representing various LULC classes within changing areas. This approach is particularly recommended in instances where Cramer's V values are low (Gibson, 2018). The results obtained from evidence likelihood are deemed satisfactory in this study, serving as a quantitative measure of the frequency of change observed between rangeland and all other land classes.

The skill measures and accuracy rates of each sub-model were calculated using MLP and SVM, and the results are summarized in Tables 6 and 7. Despite numerical data indicating a higher accuracy rate for MLP (Girma et al., 2022; Leta et al., 2021; Gharaibeh et al., 2020; Gibson et al., 2018, and others), SVM demonstrated a higher predictive ability in the current study. For the MLP sub-model, accuracy varies from 20.06% to 64.63%, while for SVM, its value fluctuates from 47.82% to 83.85%.

Table 6. Sub-models included in MLP with associated performance indicators

Sub-model	Transition/Persistence class	Minimum cells that transitioned/persisted	Class skill measure (ratio)	Sub-model accuracy, %	Sub-model skill	RMSE	
						Training	Testing
Afforestation	*Transition to the forest-covered land*: Agricultural land Bare ground Rangeland *Persistence*: Agricultural land Bare ground Rangeland	195508 15514	0.4233	51.94	0.0628 0.1816 0.4124 0.3957 0.9090 0.5762	0.3080	0.3083
Urbanisation	*Transition to built-up areas*: Forest Agricultural land Bare ground Rangeland *Persistence*: Forest Agricultural land Bare ground Rangeland	48112 15514	0.4784	54.36	-0.1429 0.5596 0.7525 0.9157 0.4597 0.5038 0.0304 0.7410	0.2659	0.2666
Flood intensification	*Transition to water and flooded areas*: Flooded areas* Agricultural land** Rangeland** *Persistence*: Flooded areas Agricultural land Rangeland	94899 3237518	0.5756	64.63	0.5851 0.7067 0.7825 0.4308 0.5319 0.4182	0.2862	0.2866
Desolation	*Transition*: Agricultural land to water Agricultural land to forest Agricultural land to flooded areas Agricultural land to built-up areas *Persistence*: Agricultural land	48112 12133	0.0008	20.06	-0.2500 1.0000 -0.2500 -0.2500 -0.2500	0.4472	0.4472

Note: * - transition to water; ** - transition to flooded areas.

Table 7. Sub-models included in SVM with associated performance indicators

Sub-model	Transition//Persistence class	SV number	CV accuracy	Out-of-sample accuracy	Skill measure
Afforestation	*Transition to the forest-covered land:*				
	Agricultural land	1637	0.7248	0.7345	0.4689
	Bare ground	1063	0.6540	0.6656	0.3312
	Rangeland	1863	0.6824	0.6716	0.3432
	Persistence:				
	Agricultural land	1648	0.6348	0.6300	0.2600
	Bare ground	1080	0.9264	0.9111	0.8223
	Rangeland	1881	0.5468	0.5294	0.0588
Urbanisation	*Transition to built-up areas:*				
	Forest				
	Agricultural land	840	0.9056	0.9149	0.8299
	Bare ground	1664	0.9104	0.9005	0.8010
	Rangeland	490	0.8400	0.8486	0.6972
	Persistence:	735	0.9100	0.9150	0.8301
	Forest				
	Agricultural land	879	0.7652	0.7772	0.5544
	Bare ground	1664	0.5924	0.5841	0.1683
	Rangeland	502	0.9700	0.9664	0.9328
		736	0.8148	0.8036	0.6072
Flood intensification	*Transition to water and flooded areas:*				
	Flooded areas*	1519	0.8268	0.8266	0.6533
	Agricultural land**	894	0.8088	0.8013	0.6026
	Rangeland**	1328	0.7816	0.7862	0.5724
	Persistence:				
	Flooded areas	1530	0.5712	0.5707	0.1414
	Agricultural land	904	0.8448	0.8355	0.6709
	Rangeland	1369	0.6932	0.6759	0.3517
Desolation	*Transition*:				
	Agricultural land to water	2200	0.2900	0.2474	0.0593
	Agricultural land to forest	2293	0.6208	0.6170	0.5213
	Agricultural land to flooded areas	1623	0.6212	0.6963	0.6204
	Agricultural land to built-up areas	1836	0.6100	0.5855	0.4819
	Persistence:				
	Agricultural land	2292	0.2492	0.2501	0.0626

Both SVM and MLP are commonly used machine learning algorithms for classification tasks, including LULC change prediction. The choice of algorithm can depend on various factors, and the fact that SVM demonstrated higher accuracy than MLP may be influenced by several reasons: (1) SVM is known for its effectiveness in handling high-dimensional data and complex decision boundaries. Considering that our LULC change prediction task involves a non-linear and complex relationship between input features, SVM performs better than MLP; (2) SVM can be more robust when dealing with small datasets. In the current study, the dataset is limited (considering dependent variables for 5 years), and due to this, SVM generalizes better than MLP, which could be more prone to overfitting; (3) the performance of both SVM and MLP heavily depends on parameter tuning. It's possible that the hyperparameters of the SVM were tuned more effectively for this specific dataset, leading to better performance; (4) SVM is effective in high-dimensional spaces and excels in capturing complex relationships, while MLP might require more data to effectively train its parameters, especially when dealing with a high-dimensional feature space; (5) SVM is generally robust to outliers present in the dataset, and it can utilize the kernel trick to transform the input space into a higher-dimensional space, making it more adaptable to non-linear relationships. It's important to note that the performance of machine learning algorithms is highly dataset-dependent, and utilizing SVM is more effective for small datasets than employing MLP. The higher accuracy is demonstrated by the model with the following parameters (Table 8).

Table 8. Model parameters and accuracy

Parameter	Value
Modelling approach	SVM learning algorithm
Sub-model	Urbanization
Kernel type	Radial Basis Function
Epsilon (ε)	0.0100
Class number	8
Total CV number	7510
Total sample number	20000
Overall CV accuracy	0.8385
Overall out-of-sample accuracy	0.8388
Overall skill measure	0.6776

Note: CV - cross-validation.

To validate the model, the Kappa statistic (k-index) for quantity and location was computed by comparing the hard simulation with the reference map of 2022 (Table 9).

Table 9. The k-index values of the simulated LULC map of 2022

Index	Value
K_{no}	0.9695
$K_{location}$	0.9724
$K_{locationStrata}$	0.9724
$K_{standard}$	0.9547

The statistics reveal that all kappa index values surpass the satisfactory range (≥ 80%). The overall disagreement between the reference and predictive maps is generally low, primarily attributed to allocation errors (0.0160) rather than quantity errors (0.0107). Despite the presence of allocation errors, the overall agreement between the actual and simulated maps is high, reaching 97.34% (Figure 6). The validation and assessment of the results from the simulation of (LULC) changes were conducted using the ROC curve to evaluate prediction accuracy. The area under the ROC curve serves as an indicator of the forecasting model's ability to correctly anticipate the occurrence or non-occurrence of pre-defined 'events' (Arora et al., 2021; Myslyva et al., 2023).

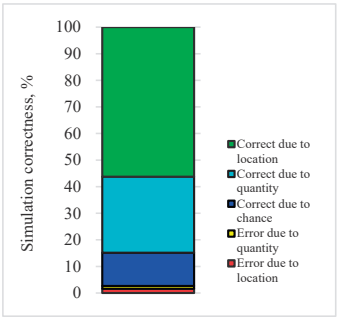

Figure 6. Successes and errors of the simulation

The model's prediction rate has been computed and is depicted in Figure 7.

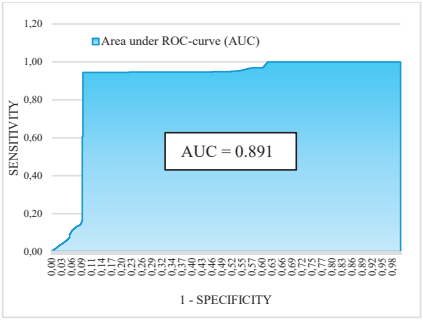

Figure 7. Performance of the model based on SVM for the LULC change prediction

The predictive model demonstrates an accuracy of 89% (AUC = 0.891), indicating a 'very good' performance level. The developed model was then used to predict future land use and land cover (LULC) changes in 2026 and 2031 under the business-as-usual (BAU) scenario.

The simulated area extent, gains, losses, and net change (in hectares) are depicted in Figures 8-10.

Notably, in the context of land use land cover modelling, a business-as-usual scenario involves projecting future land use patterns based on the assumption that current trends and practices persist without significant alterations.

Considering this, the expansion of built-up areas (8.6% and 8.3%) is expected by 2026 and 2031, respectively. In contrast, the forest-covered area (0.1%), agricultural land (0.7%), and rangeland (0.4%) are expected to decrease, while bare ground will experience a decrease until 2026 (23.4% of the area) and subsequent growth of 3.7% by 2031.

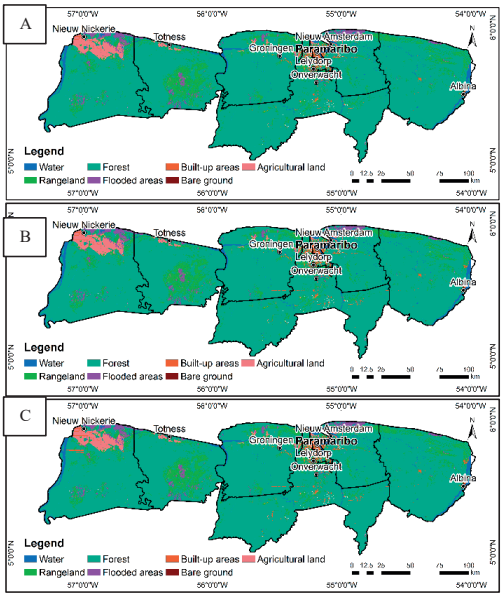

Figure 8. Existing (A) LULC map for 2022 and projected LULC maps for 2026 (B) and 2031 (C)

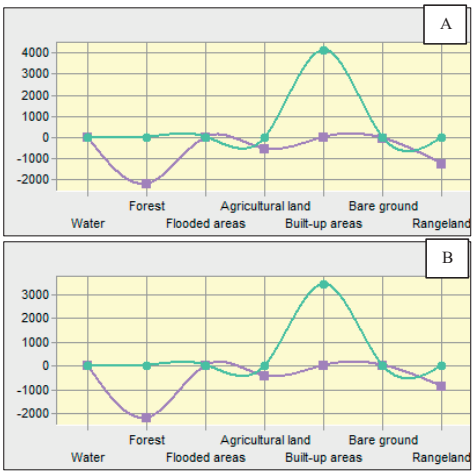

Figure 9. Gains and losses (ha) graph between 2022-2026 (A) and 2026-2031 (B)

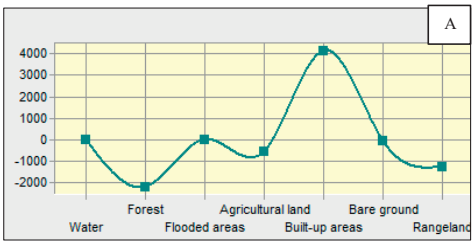

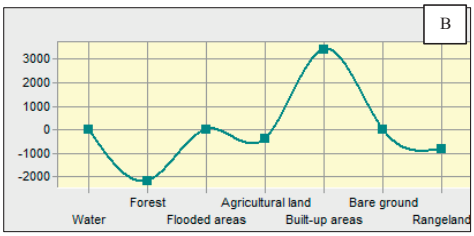

Figure 10. Net change (ha) graph between 2022-2026 (A) and 2026-2031 (B)

The forecast indicates that the Wanica and Nickerie districts will experience the most significant changes, while minor LULC changes are expected in Para and Marowijne. In general, two significant trends will be observed in the upcoming 10-year period. One involves the drastic expansion of urbanization, and the second is associated with deforestation and the shortage of agricultural land (Table 10).

Table 10. Descriptions and explanations for observed trends in LULC changes (2022-2031 predictions)

LULC class	Trend	Explanation	Required activities
Water and flooded areas	The water area will remain constant	A stable water area indicates a consistent presence of water bodies, such as rivers, lakes, and coastal areas. This stability is vital for maintaining ecosystem health and supporting various aquatic life forms	Sustainable water management practices are crucial to support wetland ecosystems
Forest	The forest area will gradually decline (net changes will amount to 0.1%)	Forest reduction is influenced by logging and infrastructure development	Sustainable forestry management practices are crucial to balance conservation efforts and economic activities
Agricultural land	Agricultural land will decrease slightly (net changes will amount to 0.7%)	This trend indicates a shift in land use due to urbanization	Supporting the balance between food production needs and environmental conservation is essential
Built-up areas	Built-up areas will significantly increase (net changes will amount to more than 8.0%)	The substantial growth in built-up areas signals urbanization and infrastructural development which drives the expansion of residential, commercial, and industrial spaces	Implementing crucial measures, such as sustainable urban planning practices, enforcing zoning regulations and engaging local communities in decision-making, is essential
Bare ground	The bare ground will fluctuate (an annual decrease of 23% for 2022–2026 and, an annual increase of 4% for 2026-2031)	Fluctuations in bare ground could result from natural processes like erosion, reforestation efforts, or human activities	Monitoring and managing bare ground are essential for preventing soil degradation and maintaining ecosystem health
Rangeland	Rangeland will gradually decrease (net changes will amount to more than 0.4%)	The decline in rangeland is influenced by factors such as urban expansion or changes in land use practices	Sustainable land management strategies are crucial to balance urban expansion with the preservation of natural habitats

Considering that Suriname faces a significant shortage of land resources suitable for building, infrastructure development, and agricultural activity, coupled with the continued use of the most productive land parcels for building construction, there is a pressing need to implement an urgent land management plan. Such a plan will help mitigate the negative consequences of irrational land use during the last decade.

CONCLUSIONS

The transformation in land use and land cover within the coastal plain area of Suriname from 2017 to 2031 was simulated using various geospatial methodologies alongside the SVM machine learning algorithm. This research utilized a range of dependent/driver and independent spatial datasets. TerrSet software was employed for assessing LULC changes, including statistical and graphical analyses of gains, losses, and net changes.

Topographical features, proximity variables, and evidence likelihood (related to the transition from rangeland to other land classes) were identified as the primary drivers of LULC change. Evidence likelihood is the most influential parameter, while distance from roads has the least effect in this study. To enhance the accuracy of future predictions, it is advisable to expand the list of independent variables to include additional information, such as weather data. When considering scenarios other than business-as-usual, it becomes necessary to augment the list of driving variables with geospatial data corresponding to the distance from deforested areas and areas with illegal mining.

Two machine learning algorithms, MLP and SVM, were tested for their ability to predict LULC change. To evaluate the accuracy and reliability of MLP and SVM algorithms-based predictive models, skill measures and accuracy rates were utilized. The SVM algorithm-based predictive model, which included the urbanization transition sub-model (bare ground, agricultural land, rangeland, and forest converted to built-up areas), demonstrated an overall skill of 0.7 and an accuracy of 83.85%. It's important to note that the performance of machine learning algorithms can be highly dataset-dependent, and the superiority of one algorithm over another may vary across different applications and datasets.

The prediction results for 2022 from the SVM algorithm-based model were further validated using the VALIDATE and ArcSDM modules, based on the actual reference image (2022). The

derived Kappa statistics (95%) and AUC value (89%) ensure the reliability of the SVM algorithm-based model in predicting land use changes. Future LULC changes for 2026 and 2031 were forecasted, considering the business-as-usual scenario. The model predicts an expansion of built-up areas between 2026 and 2030, accompanied by a reduction in forest, agricultural land, and rangeland.

Given that individual districts in Suriname possess distinct characteristics that can significantly influence future land use change predictions, forthcoming studies should undertake an examination to develop more detailed tailored predictive models. These models should encompass specific driving variables that are highly significant for each respective district

REFERENCES

Aitkenhead, M. J., Aalders, I. H. (2009). Predicting land cover using GIS, Bayesian and evolutionary algorithm methods. *Journal of Environmental Management*, 90(1), 236–250.

Anurag, Saxena, A., & Pradhan, B. (2018). Land use/ land cover change modelling: issues and challenges. *Journal of Rural Development*, 37(2), 413–424.

Arabameri, A., Rezaei, K., Cerda, A., Conoscenti, C., Kalantari, Z. (2019). A comparison of statistical methods and multi-criteria decision-making to map flood hazard susceptibility in Northern Iran. *Science of the Total Environment*, 660, 443–458.

Arora, A., Pandey, M., Siddiqui, M. A., Haoyuan, H., Mishra, V. N. (2021). Spatial flood susceptibility prediction in Middle Ganga Plain: comparison of frequency ratio and Shannon's entropy models. *Geocarto International*, 36(18), 2085–2116.

Devi, A. R., Shimrah, T. (2023). Modelling LULC using Multi-Layer Perceptron Markov change (MLP-MC) and identifying local drivers of LULC in the hilly district of Manipur, India. *Environmental Science and Pollution Research International*, 30(26), 68450–68466.

Dey, N. N., al Rakib, A., al Kafy, A., Raikwar, V. (2021). Geospatial modelling of changes in land use/land cover dynamics using multi-layer perception Markov chain model in Rajshahi City, Bangladesh. *Environmental Challenges*, 4, 100148.

Eastman, J. R. (2016). TerrSet Manual, Geospatial Monitoring and Modeling System. Clark University, Worcester, USA. Clark University, Worcester, USA.

Gardi, C., Angelini, M., Barceló, S., Comerma, J., Cruz Gaistardo, C. and all (2015). Soil Atlas of Latin America and the Caribbean. European Commission, Luxembourg, 176.

Gharaibeh, A., Shaamala, A., Obeidat, R., Al-Kofahi, S. (2020). Improving land-use change modelling by integrating ANN with cellular automata-Markov chain model. *Heliyon*, 6.

Gibson, L., Munch, Z., Palmer, A., Mantel, S. (2018). Future land cover change scenarios in South African grasslands – implications of altered biophysical drivers on land management. *Heliyon*, 4 (7).

Girma, R., Fürst C., Moges A. (2022) Land use land cover change modelling by integrating the artificial neural network with cellular Automata-Markov chain model in Gidabo river basin, main Ethiopian rift. *Environmental Challenges*, 6, 100419.

Huisden, C. M., Kanhai, S., Bogor, D. (2020). An assessment of volatile organic compound pollution in relation to the petroleum industry in Suriname. *Academic Journal of Suriname*, (11)1, 33–44.

Huisden, C. M., Landburg, G., Niram, A., Algoe, S., Dakriet, N. (2020) Mercury toxicity through fish consumption in Paramaribo, Suriname. *Academic Journal of Suriname*, (11)1, 25–32.

Hyandye, C., Geoffrey Mandara, C., Safari, J. (2015). GIS and logit regression model applications in land use/land cover change and distribution in Usangu catchment. *American Journal of Remote Sensing*, 3(1), 6–16.

Kafy, A.-A., Naim, M. d. N. H., Subramanyam, G., Faisal, A.-A., Ahmed, N. U., al Rakib, A., Kona, M. A., Sattar, G. S. (2021). Cellular Automata approach in dynamic modelling of land cover changes using RapidEye images in Dhaka, Bangladesh. *Environmental Challenges*, 4, 100084.

Leta, M. K., Demissie, T. A., Tränckner, J. (2021). Modelling and prediction of land use land cover change dynamics based on land change modeller (Lcm) in Nashe watershed, upper Blue Nile basin, Ethiopia. *Sustainability*, 13.

Marquez, A.M., Guevara, E., & Rey, D. (2019). Hybrid model for forecasting of changes in land use and land cover using satellite techniques. *IEEE Journal of Selected Topics in Applied Earth Observations and Remote Sensing*, 12, 252–273.

Mishra, V. N., Rai, P. K., Prasad, R., Punia, M., Nistor, M.–M. (2018). Prediction of spatiotemporal land use/land cover dynamics in rapidly developing Varanasi district of Uttar Pradesh, India, using geospatial approach: a comparison of hybrid models. *Applied Geomatics*, 10(3), 257–276.

Mohamed, A., Worku, H. (2020). Simulating urban land use and cover dynamics using cellular automata and Markov chain approach in Addis Ababa and the surroundings. *Urban Climate*, 31, 100545.

Muhammad, R., Zhang, W., Abbas, Z., Guo, F., Gwiazdzinski L. (2021). Spatiotemporal change analysis and prediction of future land use and land cover changes using QGIS MOLUSCE plugin and remote sensing big data: A case study of Linyi, China. *Land*, 11(3), 419.

Myslyva, T., Nadtochiy, P., Bilyavskyi, Y., & Trofymenko, P. (2023). Intra-field spatial heterogeneity prediction for the purposes of precision farming: Comparison of frequency ratio and Shannon's entropy models. Scientific Papers. Series A. *Agronomy*, LXVI (1), 138–147.

Myslyva, T., Sheliuta, B., Bushueva, V. (2021) Use of medium and high-resolution remote sensing data and Markov chains for forecasting productivity of non-conventional fodder crops. Scientific Papers. Series A. *Agronomy*, LXIV (1), 478–485.

Nhu V.-H., Shirzadi A., Shahabi H., S. K., Al-Ansari N., Clague J. J. and all (2020). Shallow landslide susceptibility mapping: a comparison between logistic model tree, logistic regression, naïve Bayes tree, artificial neural network, and support vector machine algorithms. *Environmental Research and Public Health*, 17, 2749.

Ouboter, P. E., Jairam, R. (2012). Geography of Suriname. In Amphibians of Suriname. Leiden, Netherlands: Brill, 376 pp.

Ralha, C. G., Abreu, C. G., Coelho,C. G. C., Zaghetto, A., Macchiavello, B., Machado R. B. (2013). A multi-agent model system for land-use change simulation. *Environmental Modelling and Software*, 42, 30–46.

Regasa, M. S., Nones, M., Adeba, D. (2021). A review on land use and land cover change in Ethiopian basins. *Land*, 10 (10), 585.

Rongqun Z., Chengjie T., Suhua M., Hui Y., Lingling G., Wenyu F. (2011). Using Markov chains to analyze changes in wetland trends in arid Yinchuan Plain, China. *Mathematical and Computer Modelling*, 54 (3–4), 924–930.

Rozario, P. F., Oduor, P., Kotchman, L. and Kangas, M. (2017) Transition modelling of land-use dynamics in the Pipestem Creek, North Dakota, USA. *Journal of Geoscience and Environment Protection*, 5, 182–201.

Sinha, P., Kumar, L. (2013). Markov land cover change modelling using pairs of time series satellite images. *Photogrammetric Engineering and Remote Sensing*, 79, 1037–1051.

Wang, S. W., Munkhnasan, L., Lee, W.K. (2021). Land use and land cover change detection and prediction in Bhutan's high-altitude city of Thimphu, using cellular automata and Markov chain. *Environmental. Challenges*, 2, 100017.

Yeh, C. K., Liaw, S. C. (2021). Applying spatial autocorrelation and logistic regression to analyze land cover change trajectory in a forested watershed. *Terrestrial, Atmospheric and Oceanic Sciences*, 32, 35–5.